ENVIRONMENTAL RESEARCH







LETTER • OPEN ACCESS

A hotspot and mechanism of enhanced bottom intrusion on the southern New England shelf

To cite this article: Ke Chen 2024 Environ. Res. Commun. 6 071008

View the article online for updates and enhancements.

You may also like

- Analysis of the MPL/GDL Interface: Impact of MPL Intrusion into the GDL Substrate Anne Berger, Yen-Chun Chen, Jacqueline Gatzemeier et al.
- Evaluating a potential technique with local optical flow vectors for automatic organ-atrisk (OAR) intrusion detection and avoidance during radiotherapy
 P Troy Teo, Kaiming Guo, Bilal Ahmed et al
- Multiple Overspill Flood Channels from Young Craters Require Surface Melting and Hundreds of Meters of Midlatitude Ice Late in Mars's History Alexandra O. Warren, Sharon A. Wilson, Alan Howard et al.



Environmental Research Communications



OPEN ACCESS

RECEIVED 9 April 2024

REVISED

1 July 2024

ACCEPTED FOR PUBLICATION

10 July 2024

PUBLISHED 23 July 2024

Original content from this work may be used under the terms of the Creative Commons Attribution 4.0 licence.

Any further distribution of this work must maintain attribution to the author(s) and the title of the work, journal citation and DOI.



LETTER

A hotspot and mechanism of enhanced bottom intrusion on the southern New England shelf

Ke Chen

Physical Oceanography Department, Woods Hole Oceanographic Institution, United States of America

E-mail: kchen@whoi.edu

Keywords: hotspots, cross-shelf exchange, bottom intrusions, pressure gradient setup, wind-driven upwelling, subsurface compound anomaly

Abstract

Understanding the occurrence of the intrusion of open ocean water onto continental shelves has scientific significance and societal relevance as the intrusion can significantly disrupt the marine ecosystem and fisheries. High-resolution numerical modeling is used to investigate the spatiotemporal occurrence and mechanisms of highly anomalous bottom intrusions on the southern New England shelf. Based on multi-year numerical simulations, this study reveals a hotspot of cross-isobath bottom-intensified intrusions at a topographic trough. Examination of multiple events portrays a robust mechanism of locally enhanced bottom intrusions. Persistent upwelling-favorable winds set up an enhanced pressure gradient field at the topographic trough and drive the intrusion a large-distance onshore. Numerical experiments with and without the topographic trough show that the localized pressure gradient results from a combination of the shelf orientation and local bathymetry. Although highly anomalous waters on the shelf relate to wind forcing, correlations between the wind stress anomaly and bottom salinity anomaly at the location of the enhanced intrusion is modest, implying the need to incorporate other environmental factors to develop more deterministic prediction models for subsurface conditions on the shelf. The results have important implications for marine environment and fisheries management.

1. Introduction

Exchanges of water masses between the coastal and open ocean have significant impacts on budgets of heat, salt, nutrient, carbon and ecosystems. On the southern New England shelf (figure 1(a)) in the northern Middle Atlantic Bight (MAB), the intrusions of warm and salty slope water onto the continental shelf can manifest as surface intrusions, mid-depth salinity max (Smax) intrusions (Gordon and Aikman 1981, Churchill 1985, Lentz 2003, Gawarkiewicz et al 2022), and bottom intrusions (Boicourt and Hacker 1976, Lentz et al 2003, Ullman et al 2014). Besides altering the physical environment, cross-shelf intrusions also have significant impact on the ecosystem and fisheries, particularly bottom intrusions as onshore bottom flow would drive larger nutrient fluxes (e.g., Hales et al 2009) and alter near bottom temperature, which many commercially valuable marine species (e.g., scallop, lobster) are sensitive to.

Previous field studies in the region such as the Nantucket Shoals Flux Experiment (NSFE, Beardsley *et al* 1985), the Shelf Edge Exchange Program (SEEP-1, Houghton *et al* 1988), and Coastal Mixing and Optics (CMO, Lentz *et al* 2003) have shown that cross-shelf near bottom intrusions resulting from the onshore migration of the shelfbreak front can be driven by upwelling-favorable wind. Due to dynamical constraints, the migration distance is typically within $10-20 \, \mathrm{km}$ from the shelfbreak (Lentz *et al* 2003). However, recent observations reveal two highly anomalous large-magnitude cross-shelf intrusions on the Southern New England shelf. The first one occurred when anomalous warm and salty water intruded into the Rhode Island Sound (30 m–50 m isobaths, $\sim 100 \, \mathrm{km}$ inshore of the shelfbreak) in late fall of 2009, as revealed by mooring data and shipboard hydrography



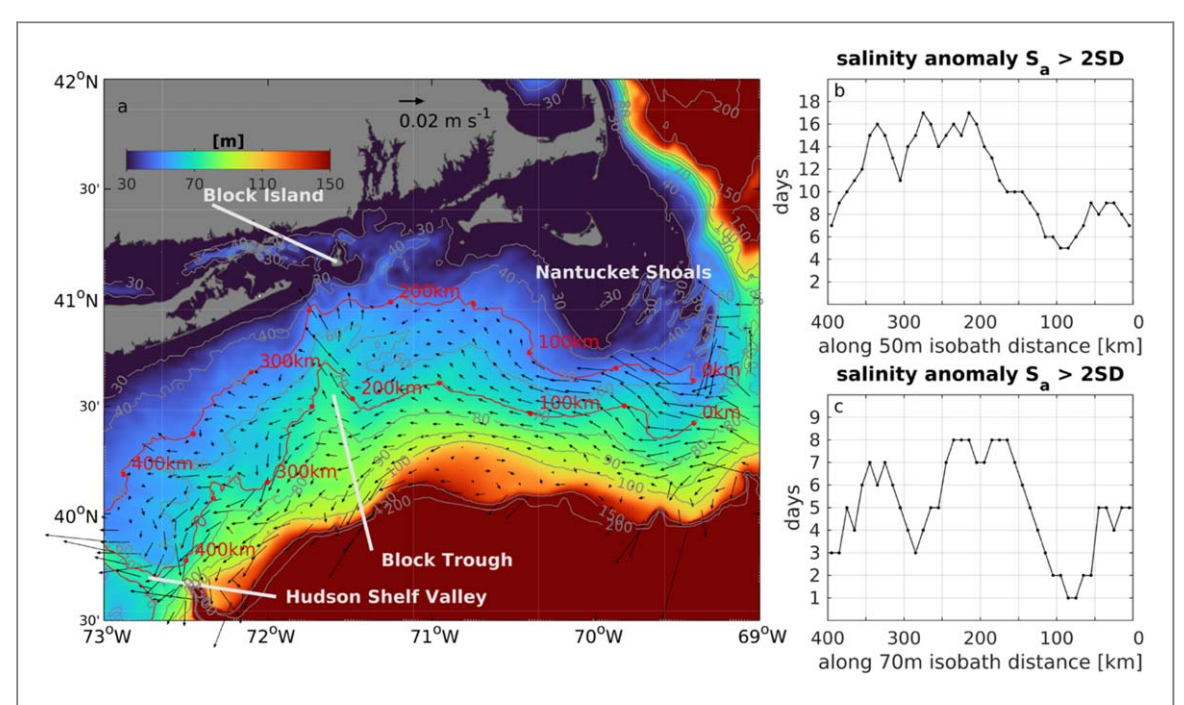


Figure 1. (a) Map showing the southern New England continental shelf. Bathymetry is shown in color with a range from 30 m to 150 m isobath. The selected isobaths are further contoured in gray. The 50 m and 70 m isobaths from the model are contoured in red, with along-isobath distance from the upstream end marked (with red dots, along-isobath spacing 50 km). The black vectors denote the eight-year mean bottom velocity between the 50 m and 150 m isobaths, i.e., mid- to outer shelf. Relevant geographic locations are labelled. (b) Days per year when the bottom salinity anomaly exceeds two standard deviations along the 50 m isobath (c) Same as (b) but for the 70 m isobath. Along-isobath resolution in (b) and (c) is 10 km.

measurements (Ullman *et al* 2014). The authors noted that salinity in November-December 2009 was substantially higher (by 1 psu) than all existing historical hydrographic data within 25 km of their study site. The second intrusion was detected by observations collected by commercial fishing vessels as part of a community science program (Gawarkiewicz and Mercer 2019) in January 2017 over the southern New England shelf. Anomalies of the depth-averaged temperature and salinity exceeded 4 °C and 1 psu respectively, both above the 97th percentile of all historical profiles in the same region (Gawarkiewicz *et al* 2019). The anomalous water properties in January 2017 were accompanied by unusual distributions of fish and invertebrate species over the continental shelf, impacting the productivity of commercial fishing activities in the region.

Combining available observations and a high-resolution (1-km) numerical model in a realistic configuration, Chen *et al* (2022) showed that offshore eddies and upwelling-favorable wind were responsible for driving a cross-shelf bottom intrusion leading to highly anomalous water properties toward the inner shelf. Distinct from a 2D wind-driven conceptual model, along-shelf bathymetry plays an important role in shaping the bottom intrusion: the intrusion is enhanced at a topographic trough where local isobaths also change orientation. While this case study identified the importance of wind forcing, offshore preconditioning and along-shelf variation of bathymetry in driving significant water mass anomalies, the relevance of these ingredients in bottom intrusions over different oceanographic conditions deserves further investigations. For example, does the local bathymetry make certain places over the southern New England shelf hot spots for cross-shelf exchange? Or, how deterministic is upwelling wind in driving localized cross-isobath intrusions given realistic bathymetry? Answering these questions will improve our understanding of processes driving large-magnitude cross-shelf bottom intrusions, which as stated above is both scientifically important and broadly relevant.

This study seeks to better understand the characteristics of the spatial and temporal occurrence of enhanced bottom intrusions and the associated mechanisms on the southern New England shelf. The approach is to examine large-magnitude bottom intrusions in multiple years using the same Northeast Shelf and Slope (NESS) model as in Chen *et al* (2022).

2. Numerical modeling

The numerical model is the NESS primitive equation model developed for the Northeast U.S. shelf and slope region based on the hydrostatic Regional Ocean Modeling System (ROMS). It has 1-km horizontal resolution and 40 vertical terrain-following layers. This high-resolution is essential in capturing mesoscale-submesoscale



processes from the Gulf Stream to the coastal ocean and detailed bathymetric features, both of which were important in producing the large magnitude cross-shelf bottom intrusion in 2017 (Chen *et al* 2022). For more technical details and numerical treatments, the readers are referred to the description in Chen *et al* (2022).

An eight-year control hindcast is conducted from 2010 to 2017. The model, which is configured in the same way as that in Chen *et al* (2022), has been shown to be capable of resolving relevant processes and compares well with observations. Point-to-point comparison with Commercial Fisheries Research Foundation (CFRF)— Woods Hole Oceanographic Institution (WHOI) hydrographic data (Gawarkiewicz and Mercer 2019) confirms a similar model performance as that in Chen *et al* (2022) (not shown). In addition to the control run, one experiment with no topographic trough over the southern New England shelf is also conducted. In this experiment, the topographic trough is removed so the effect of the shallow trough can be isolated. Specifically, the 30 m to 100 m isobaths between 72° 54′ W and 71° 24′ W is modified so that the no bathymetric features exist except the general orientation of isobaths following the shelf direction (section 3.3 for details).

3. Results

3.1. Spatial characteristics of the bottom intrusion

The eight-year mean bottom currents over the mid- to outer shelf are, to the lowest order, along-isobath (figure 1(a)). However, obvious cross-isobath flows can be identified, most notably at the topographic trough (referred to as Block Trough, to be consistent with Block Island and Block Canyon) over the southern New England shelf (between 72° W and 71° W) as well as the Hudson Shelf Valley ($\sim 73^{\circ}$ W). The mean bottom currents reflect the sum of various forcings over different stratification conditions, e.g., buoyancy-driven along-shelf flow, upwelling- and downwelling-favorable winds. For the Hudson Shelf Valley, it has been known that the mean flows over time scales of months tend to be onshore, presumably due to the asymmetry of the response of along-valley flow to winds (Lentz et al 2014, Zhang and Lentz 2017). In comparison, bottom flow patterns around the Block Trough have not been well documented. Dedicated observations, particularly velocity measurements in the area, are absent and many numerical models (both global and regional) do not sufficiently represent the detailed bathymetric features and circulation in the region.

Along-isobath distribution of the salinity anomalies reveal the spatially varying cross-shelf exchanges along the bottom as the mean bottom current pattern indicates (figures 1(b), (c)). The calculations are done for each 10 km segment along the 50 m and 70 m isobaths from 2010 to 2017. For each segment, the daily climatological mean and standard deviations are calculated for each year day using bottom salinity values within a 15-day window. Along the 70 m isobath, the frequency of bottom salinity exceeding two standard deviations varies from 1 to 8 days per year (figure 1(c)). The occurrence of high salinity anomalies is more frequent between 150 km and 250 km, around the Block Trough and its northern flank, with a frequency of 8 days per year. That is 60% more frequent than that of the areal mean occurrence (5 days per year), or seven times more frequent than regions of lowest occurrence. Another location of frequent high salinity anomalies is between 300 km and 350 km at the 70 m isobath, where a mild topographic depression is located (between 72°30′ W and 72° W, figure 1(a)). Similarly, along the 50 m isobath, large bottom salinity anomalies can be more frequently found between 200 km and 300 km, around the head (inshore end) of the Block Trough. The frequency of occurrence is ~ 17 days per year, which is also ~60% more than the mean frequency along the 50 m isobath, or more than double the frequency at the region of lowest occurrence, to the south of the Nantucket Shoals. A secondary region of frequent occurrence along the 50 m isobath is at \sim 350 km, close to the head of another mild topographic depression. In combination, the results indicate a higher frequency of anomalous bottom salinity at topographic depressions at the mid- to outer southern New England shelf, making them hot spots for bottom intrusions. In the following, we focus on the Block Trough extending from the outer shelf toward the Block Island, which is the same region where the 2017 bottom intrusion developed.

3.2. Composite analysis of circulation and momentum

The representativeness of the 2017 bottom intrusion is examined by extracting events with high salinity anomalies over multiple years. Focusing on the Block Trough, events with salinity anomalies exceeding two standard deviations are selected to produce composite mean fields. Over the eight-year simulation from 2010 to 2017, 19 events over 11 months (except August) are identified. The bottom salinity and current fields in the composite remarkably resemble the patterns of the 2017 bottom intrusion (cf, figures 2(a), (b), and figure 15 in Chen *et al* 2022). First, the anomalous bottom salinity is clearly associated with upwelling-favorable wind, starting from \sim 6 days before the date when the salinity anomaly reaches its maximum. Second, the enhanced onshore, cross-isobath flow is concentrated at the same location along the Block Trough. Third, the cross-isobath intrusion starts earlier than the setup of the along-isobath flow. The consistency between the composite mean and the 2017 event indicates that wind forcing is a common mechanism driving intrusion flows in this



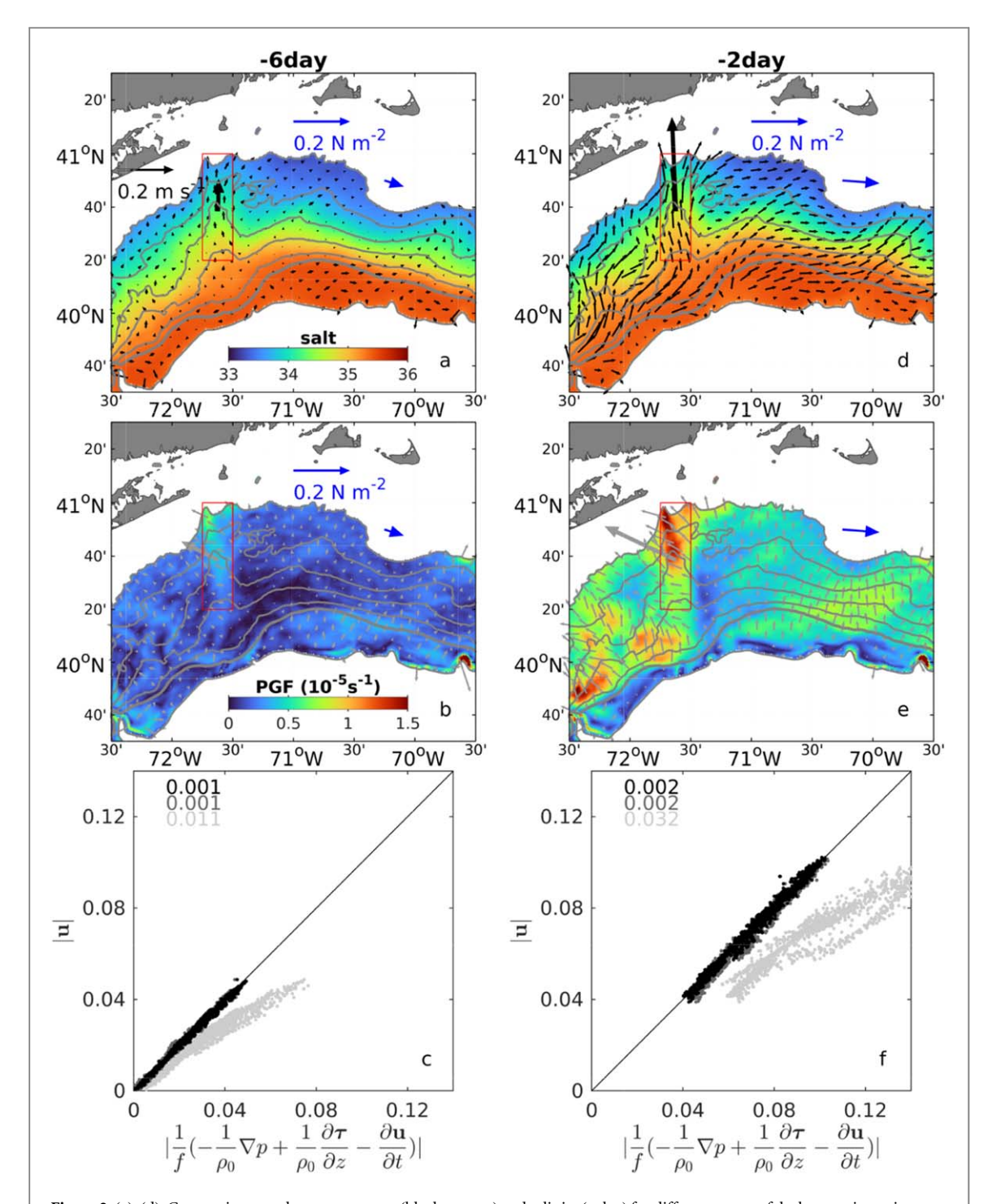


Figure 2. (a), (d): Composite mean bottom currents (black vectors) and salinity (color) for different stages of the bottom intrusion relative to the maximum salinity anomaly at the Block Trough (averaged within the rectangular box): 6 days and 2 days prior to the time of maximum anomaly. Spatial mean bottom velocity vector (within the rectangular box) is shown with magnitude amplified by five times for better visualization. Mean wind stress in the region is shown in blue vectors. (b), (e): Same as (a), (d) but for bottom pressure gradient force with magnitude in color and directions in gray vectors. (c), (f): Estimates of the bottom flow using pressure gradient, stress divergence, and acceleration terms within the trough. The light gray dots represent the geostrophic balance, i.e., using the first term to infer bottom flow. The darker gray represents the contribution of the pressure gradient and stress divergence. The black dots represent the consideration of the additional acceleration term, i.e., all three terms below the x-axis. Color-coded Root Mean Square Difference (RMSD) values are shown.

region. This is evidenced by the analysis of the momentum balance during the development of the bottom intrusion process.

The main terms in the cross-isobath and along-isobath momentum balances at a certain isobath on the shelf (e.g., the 70 m isobath) are:

$$\frac{\partial u}{\partial t} = fv - \frac{1}{\rho_0} \frac{\partial p}{\partial x} - \mathbf{u} \cdot \nabla u - w \frac{\partial u}{\partial z} + \frac{\partial}{\partial z} \left(K_v \frac{\partial u}{\partial z} \right) \tag{1}$$



$$\frac{\partial v}{\partial t} = -fu - \frac{1}{\rho_o} \frac{\partial p}{\partial y} - \mathbf{u} \cdot \nabla v - w \frac{\partial v}{\partial z} + \frac{\partial}{\partial z} \left(K_v \frac{\partial v}{\partial z} \right) \tag{2}$$

where x and y are rotated to cross-isobath (positive offshore) and along-isobath (positive poleward) directions, u and v are defined as cross-isobath (positive offshore) and along-isobath (positive poleward), f is the Coriolis parameter, ρ_0 is the mean seawater density, p is the pressure, \mathbf{u} is the horizontal velocity vector, w is the vertical velocity, and K_v is the vertical viscosity. The terms on the right-hand side of (1) and (2) are Coriolis (cor), pressure gradient force (pgf), nonlinear horizontal and vertical advection of momentum (adv), and vertical mixing of momentum, which is also the stress divergence term (str). Horizontal viscous terms are small and have been neglected. The cross- and along-isobath ageostrophic (ageo) velocities can be expressed by:

$$u_a = \left(fu + \frac{1}{\rho_o} \frac{\partial p}{\partial y} \right) / f \tag{3}$$

$$v_a = \left(f v - \frac{1}{\rho_o} \frac{\partial p}{\partial x} \right) / f \tag{4}$$

Starting from six days prior to the peak salinity anomaly, an enhanced pressure gradient sets up along the Block Trough (figures 2(b), (e)). The directions of the pressure gradient force (PGF) are directed to the northwest, facilitating northeastward cross-isobath flow toward the head of the trough.

The magnitude of the bottom velocity can be retrieved by the combination of the pressure gradient term and stress divergence (figure 2(c)), that is,

$$|\mathbf{u}| \approx \frac{1}{\rho_0 f} \left| \left(-\nabla p + \frac{\partial \tau}{\partial z} \right) \right|$$
 (5)

where ${\bf u}$ is the bottom velocity, ρ_0 is the average seawater density, f is the Coriolis parameter, p is the pressure at the sea floor, and τ is the total stress and is expressed as $\tau = K_v \frac{\partial {\bf u}}{\partial z}$. Among the three terms in equation (5), the only driving term is the pressure gradient term. As demonstrated by Chen $et\,al\,(2022)$, the setup of this pressure gradient at the Block Trough is clearly associated with upwelling-favorable winds. In other words, wind forcing sets up the pressure gradient, which drives onshore cross-isobath bottom flow balanced by near bottom stress divergence. The actual bottom flow is weaker than the geostrophic velocity due to the presence of bottom friction (figure 2(c)).

The composite analysis shows a consistent upwelling-favorable wind pattern leading to the peak salinity anomaly. A similar circulation pattern appears two days before the peak anomaly (figure 2(d)). At this stage, regional scale along-isobath flow develops, with more pronounced onshore flow at the Block Trough. The horizontal momentum is still largely balanced between Coriolis, pressure gradient, and stress divergence terms (figure 2(f)). In comparison to the first stage (6 days prior the peak anomaly), all terms are about twice as large, consistent with the stronger wind stress. Throughout, nonlinear advection of momentum is not important, which is different from the numerical studies of Hudson Shelf Valley or canyon circulation in general (e.g., Allen and Durrieu de Madron 2009, Zhang and Lentz 2018). This is because the Rossby Number at the Block Trough is small, that is, Ro = U/fL is ~ 0.05 , where U is the magnitude of the flow field ($\sim 0.1 \text{ m s}^{-1}$), and L is the characteristic width of the trough ($\sim 20 \text{ km}$). The smaller Rossby number implies different dynamical processes operating at the Block Trough from more topographically influenced canyon and valley flows.

3.3. Setup of the pressure gradient field

The setup of enhanced pressure gradient field at the Block Trough is one salient feature both for the 2017 event (Figure 17 in Chen *et al* 2022) and the composite analysis. Observational and numerical studies have discussed the importance of the pressure gradient in circulation at continental canyons and valleys (e.g., Klinck 1996, Allen 2000, Yuan 2002, Lentz *et al* 2014). As the pressure gradient can both represent the driving force and reflect the strength of geostrophic flow as a diagnostic variable, the role of the pressure gradient needs to be elucidated. In the early stage of the development of a bottom intrusion, the broad-scale pressure gradient sets up in response to the upwelling-favorable wind field (figure 2(b)). For the 2D wind-driven model, this pressure gradient would drive along-shelf flow in the direction of the wind; the along-shelf flow further drives bottom Ekman flow onshore. However, with realistic coastline and bathymetry, the magnitudes and directions of the pressure



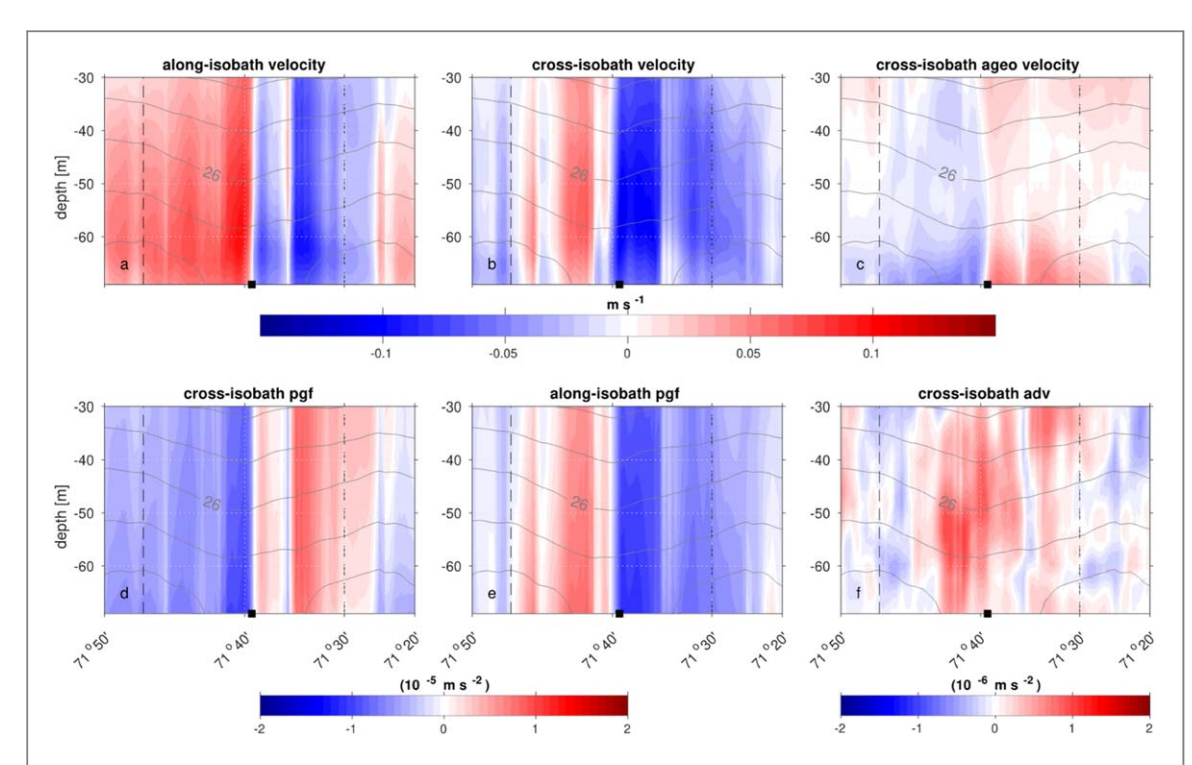


Figure 3. Along- and cross-isobath velocity and momentum terms at the 70 m isobath: (a) along-shelf velocity, (b) cross-isobath velocity, (c) cross-isobath ageostrophic velocity, (d) cross-isobath pressure gradient force, (e) along-isobath pressure gradient force, and (f) cross-isobath momentum advection. Only the segment around the Block Trough and the lower water column are shown. Density contours are shown in gray. The black dashed lines denote the longitudinal boundary defining the trough in figures 2 and 4. The black square denotes the longitude of the head of the Block Trough at the 70 m isobath. For along-isobath (cross-isobath) terms, positive direction is defined poleward (offshore). Note horizontal axis is plotted in distance but labelled in longitude. Also note the different color scales used.

gradient are by no means spatially homogenous. Larger magnitude pressure gradient force can be found at the trough (figure 2(b)).

The enhanced pressure gradient setup is a convoluted result of local circulation dynamics and topographic features. In response to upwelling-favorable wind, along-isobath geostrophic flow develops in the downwind direction. Approaching the head of the trough ($\sim 71^{\circ} 40'$), the along-isobath flow yeers to the direction of the larger-scale pressure gradient force. In addition, the local isobaths converge toward the head of the trough. The alignment of pressure gradient force and along-isobath flow as well as the convergence of isobaths would favor the acceleration of the along-isobath geostrophic flow (e.g., Klinck 1996, Allen 2000). This is clearly the case for along-isobath flow on the left flank of the trough (more positive velocity in figure 3(a)). Correspondingly, there is also enhanced cross-isobath pressure gradient force as a result of the geostrophic balance, which leads to the enhanced pattern locally (enhanced negative pgf values in figure 3(d); figure 4(a)). Accompanying the acceleration of the along-isobath flow is also the along-isobath stress (not shown) and cross-isobath advection of momentum (figure 3(f)). The enhanced stress term near bottom drives an onshore ageostrophic (bottom Ekman) flow along the left flank of the Block Trough (negative ageo values in figure 3(c)). The advection of momentum in the cross-isobath direction, despite its overall smaller magnitude, becomes more important approaching the head of the trough, which further breaks down the cross-isobath geostrophic balance and enables cross-isobath flow. In the meantime, the turning isobath at the curvature of the 70 m isobath facilitates cross-isobath flow. Due to the curvature of the local isobath, the enhanced cross-isobath pressure gradient manifests into along-isobath pressure gradient to the east (right) of 71° 40' (enhanced negative pgf values in figure 3(e); figure 4(a)). This broad-scale pressure gradient force drives significant cross-isobath flow (figure 3(b)). The cross-isobath ageostrophic velocity, which reflects the imbalance between the along-isobath pressure gradient and Coriolis terms, is positive or offshore at the eastern flank of the trough (positive values of ageo to the east (right) of 71° 40′ in figure 3(c)), which compensates the net onshore flow. According to

equation (3), this means that the magnitude of the pressure gradient force $\left| -\frac{1}{\rho_o} \frac{\partial p}{\partial y} \right|$ exceeds that of the Coriolis and drives the onshore bottom-intensified flow.

The pressure gradient setup at the trough is also associated with the configuration of the coastal boundary and broader scale orientation of isobaths in the region, regardless of the presence of the Block Trough. To



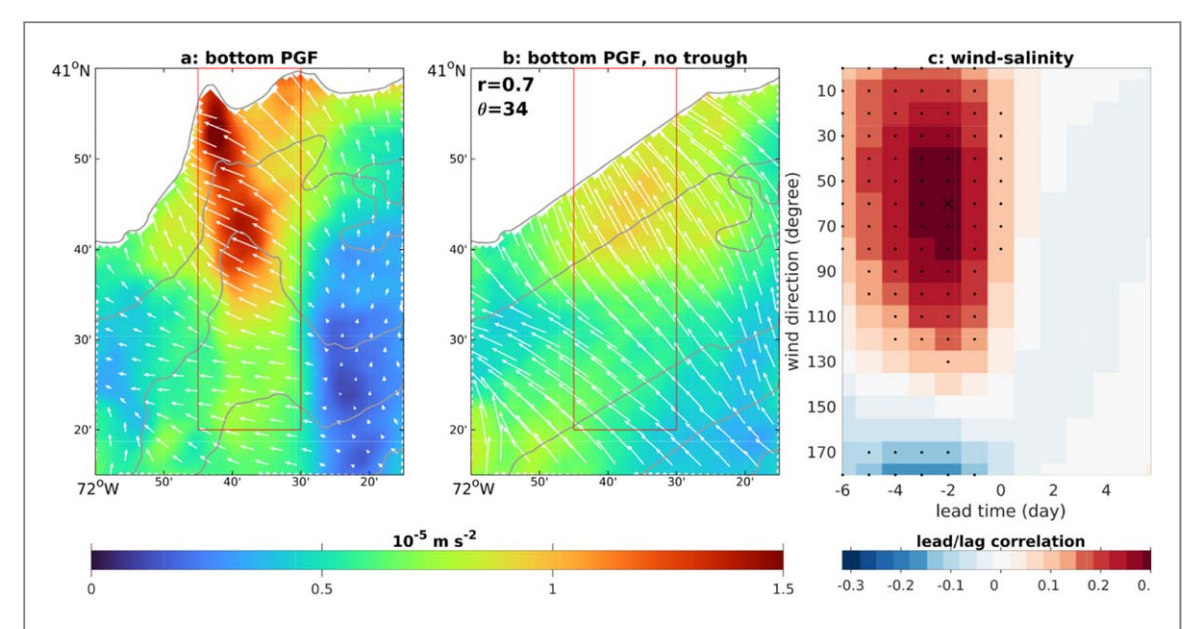


Figure 4. Pressure gradient force (PGF) at the Block Trough 2 days prior (a) to the time of maximum salinity anomaly. (b): Same as (a) but for the experiment without a topographic trough. Color represents magnitude and white vectors represent the direction of PGF. 50 m, 60 m, 70 m, 80 m, and 90 m isobaths are contoured in gray. Complex correlations of PGF fields between the control experiment and the experiment without the trough are shown in panel b with the first value being the magnitude correlation (r) and the second value being the overall angle difference (θ , both within the rectangular region). (c): Correlation between wind stress at different directions (from 0 to 180 from north) and bottom salinity at the trough. Coefficients significant above 99% confidence level are denoted by black dots with the maximum value in a black cross. Wind direction is defined as the angle clockwise from the north.

demonstrate this, one numerical experiment without the trough was conducted (see section 2). The composite pressure gradient field 2 days prior to the peak salinity anomaly roughly resembles that in the control experiment (figure 4(b)). The onshore pressure gradient force is aligned with the 2D upwelling scenario, and the location of the larger magnitude is qualitatively similar to that in the control simulation. The complex correlation between the bottom pressure gradient vectors between the two experiments reveals a magnitude correlation of 0.7 and angle difference of 34° within the predefined rectangular region. The similarity of the pressure gradient setup (larger magnitude at similar locations) is presumably determined by the common factors between the two experiments, that is, the veering orientation of the continental shelf, which would favor a higher pressure center where the west-east running isobaths intersect in the southwest-northeast direction (Chen *et al* 2022). In other words, with or without the Block Trough, higher pressure gradient can be established at approximately the same location.

3.4. Determinism of wind forcing in bottom anomaly

The composite analysis above draws a clear connection between enhanced bottom intrusion and wind forcing. Numerical experiments show that without persistent wind forcing, no bottom intrusion would occur (Chen *et al* 2022). This naturally leads to the prediction question: whether and to what extent wind can be used to predict the bottom water mass anomaly? To answer this question, lead-lag correlation between regional mean wind stress anomalies (seasonal cycle removed) on the southern New England shelf and average bottom salinity anomalies in the trough is analyzed. The results reveal significant positive correlations between upwelling-favorable winds and bottom salinity a few days later in the trough (figure 4(c)). The largest correlation is 60° T winds leading bottom salinity by 2 days, with a correlation coefficient of ~ 0.3 . While the correlation is significant above the 99% confidence level (using t-test and effective degree of freedom (Emery and Thomson 2001)) and is useful for developing prediction models, the coefficient is not particularly large, implying that other factors can help improve the prediction. For example, the preconditioning of both the shelf and slope water properties via the impingement of offshore eddies (Chen *et al* 2022) may need to be included for more deterministic predictions.

4. Summary and implications

This work investigates the spatiotemporal occurrence and dynamics of enhanced bottom intrusions on the southern New England continental shelf. An eight-year high-resolution realistic model simulation reveals that highly anomalous bottom waters driven by onshore intrusions are more frequently found at the Block Trough to



the south of the Block Island, which makes it a hotspot for bottom intrusions. Composite analysis of highly anomalous events over the eight-year simulation unravels a dominant mechanism remarkably similar to that in an earlier study of an event in 2017 (Chen *et al* 2022): the water mass anomalies are associated with cross-isobath, bottom-intensified onshore intrusions at the trough driven by persistent upwelling-favorable winds. The intrusions are driven by the enhanced pressure gradient field, which is set up by the large-scale wind forcing and modulated by the configuration of the shelf bathymetry and orientation of the coastal boundary. A similar pressure gradient setup exists in a numerical experiment without the Block Trough, implying that the relatively gentle trough is less decisive in setting up the pressure gradient field. The predictability of the bottom water mass anomalies at the trough is examined based on the cross-correlation of wind stress and bottom salinity anomalies. Statistically significant correlations can be established between the two, with maximum correlation being 60°T wind leading bottom salinity anomaly in two days. More deterministic prediction models need to incorporate other factors such as preconditioning of the shelfbreak hydrographic properties.

The study of bottom water anomalies has great implications for the marine ecosystem and fisheries. Many commercially valuable fish and shellfish species such as scallop and lobster, the two of the most valuable single species in the entire U.S., are highly sensitive to the bottom conditions on the northeast U.S. continental shelf. Future studies are needed to more comprehensively understand the similarities and differences in the characteristics and dynamics of bottom intensified intrusions under a variety of background conditions and to develop robust prediction models of subsurface ocean conditions on the continental shelf.

Acknowledgments

This work was supported by the National Oceanic and Atmospheric Administration (NOAA) Climate Program Office (CPO) Climate Variability and Predictability (CVP) program under grant NA20OAR4310398, and the National Science Foundation (NSF) Ocean Science Division under grant OCE-2241407. KC was also supported by the Woods Hole Oceanographic Institution George E Thibault Early Career Scientist Fund. Discussions with Drs. Glen Gawarkiewicz and Jiayan Yang were helpful.

Data availability statement

The data that support the findings of this study are openly available at the following URL: https://figshare.com/s/7b94d5b27d1d7abfb4d1.

ORCID iDs

Ke Chen https://orcid.org/0000-0001-8901-2996

References

Allen S E 2000 On subinertial flow in submarine canyons: effect of geometry *Journal of Geophysical Research*: Oceans 105 1285–97
Allen S E and Durrieu de Madron X 2009 A review of the role of submarine canyons in deep-ocean exchange with the shelf *Ocean Sci.* 5 607–20

Beardsley R C, Chapman D C, Brink K H, Ramp S R and Schlitz R 1985 The nantucket shoals flux experiment (NSFE79). Part 1, a basic description of the current and temperature variability *J. Phys. Oceanogr.* 15 713—48

Boicourt W C and Hacker P W 1976 Circulation on the Atlantic continental shelf of the United States, cape may to cape hatteras *Memoires de la Societe Royale des Sciences de Liege* ed J C J Nihoul (Univ. of Liege) 187–200

Chen K, Gawarkiewicz G and Yang J 2022 Mesoscale and Submesoscale shelf-ocean exchanges initialize an advective marine heatwave Journal of Geophysical Research: Oceans 127 e2021JC017927

Churchill J H 1985 Intrusions of outer shelf and slope water within the nearshore zone off long island *Limnol. Oceanogr.* 30 972–86 Emery W J and Thomson R E 2001 chapter 3 - statistical methods and error handling *Data Analysis Methods in Physical Oceanography* ed W J E E Thomson (Elsevier Science) 193–304

Gawarkiewicz G and Mercer A M 2019 Partnering with fishing fleets to monitor ocean conditions *Annual Review of Marine Science* 11 391–411

Gawarkiewicz G, Fratantoni P, Bahr F and Ellertson A 2022 Increasing Frequency of Mid-depth salinity maximum intrusions in the middle atlantic bight *Journal of Geophysical Research: Oceans* 127 e2021JC018233

Gawarkiewicz G, Chen K, Forsyth J, Bahr F, Mercer A M, Ellertson A, Fratantoni P, Seim H, Haines S and Han L 2019 Characteristics of an advective marine heatwave in the middle atlantic bight in early 2017 Frontiers in Marine Science 6712

Gordon A L and Aikman F 1981 Salinity maximum in the pycnocline of the middle atlantic bight Limnol. Oceanogr. 26 123-30

Hales B, Vaillancourt R D, Prieto L, Marra J, Houghton R and Hebert D 2009 High-resolution surveys of the biogeochemistry of the New England shelfbreak front during Summer, 2002 J. Mar. Syst. 78 426–41

Houghton R W, Aikman F and Ou H W 1988 Shelf-slope frontal structure and cross-shelf exchange at the New England shelfbreak Contiental Shelf Research 8 687–710

Klinck J M 1996 Circulation near submarine canyons: a modeling study Journal of Geophysical Research: Oceans 101 1211-23



Lentz S, Shearman K, Anderson S, Plueddemann A and Edson J 2003 Evolution of stratification over the New England shelf during the coastal mixing and optics study, August 1996–June 1997 *Journal of Geophysical Research: Oceans* 108 3008

Lentz S J 2003 A climatology of salty intrusions over the continental shelf from Georges Bank to Cape Hatteras *J. Geophys. Res.* 108 3326 Lentz S J, Butman B and Harris C 2014 The vertical structure of the circulation and dynamics in Hudson Shelf Valley *Journal of Geophysical Research: Oceans* 119 3694–713

 $\label{lem:continuous} Ullman\ D\ S,\ Codiga\ D\ L,\ Pfeiffer-Herbert\ A\ and\ Kincaid\ C\ R\ 2014\ An\ anomalous\ near-bottom\ cross-shelf\ intrusion\ of\ slope\ water\ on\ the\ southern\ New\ England\ continental\ shelf\ \textit{Journal\ of\ Geophysical\ Research:\ Oceans\ 119\ 1739-53}$

 $Yuan\ D\ 2002\ A\ numerical\ study\ of\ barotropicly\ forced\ intrusion\ in\ DeSoto\ Canyon\ \emph{\emph{J. Geophys. Res.}}\ \textbf{107}\ 2-1-2-15$

Zhang W and Lentz S J 2017 Wind-driven circulation in a shelf valley. Part I: mechanism of the asymmetrical response to along-shelf winds in opposite directions *J. Phys. Oceanogr.* 47 2927–47

Zhang W and Lentz S J 2018 Wind-driven circulation in a shelf valley: II. Dynamics of the along-valley velocity and transport *J. Phys. Oceanogr.* 48 883–904